Investigation of the Hertzsprung-Russell Diagram for Praesepe

Hyunseung Cho

Received July 05, 2023
Accepted July 01, 2024
Electronic access July 15, 2024

The Hertzsprung–Russell (H-R) diagram represents the relationship between temperature and luminosity of stars. It summarizes stellar evolution and the cycle of life of stars. It also helps us find the properties, such as radius, mass, age, and stage of evolution of individual stars and groups of stars on the H-R diagram. This paper investigates the properties of Praesepe by using the H-R diagram. Isochrone fitting was employed to estimate the cluster's age, resulting in an approximate age of 0.7 Gyr. The virial theorem was applied to determine the cluster's mass, yielding a final mass estimate of approximately 572.4 $M\odot$. Additionally, the average distance to the cluster was estimated to be 180.2552 parsecs using Gaia parallax measurements. The study also examined the cluster's stellar populations, identifying white dwarfs, giants, and supergiants, and providing insights into their relative abundances and distributions. The analysis showed the presence of five white dwarfs. This investigation of Praesepe not only validates existing data but also enhances our understanding of the cluster's stellar dynamics and evolutionary stage.

Introduction

Through this study, the physical properties of the Beehive cluster have been examined using the Hertzsprung–Russell diagram, also known as the H-R diagram. This diagram is a scatterplot that plots stars' temperature against their luminosity. The H-R diagram allows astronomers to understand more about a star's stage of stellar evolution based on the star's location on the graph. In this study, we used this diagram to find out the cluster's age, mass, and distance away from the Earth.

In the 1900s, astronomers started to understand further about stellar evolution. They understood that fusion created energy to power the stars and that the stars would eventually burn out when there was not enough fuel to use for fusion. Ejnar Hertzsprung, a Danish astronomer, created a graph of stars' color to luminosity in 1911. Luminosity is the measure of electromagnetic radiation emitted by a star per amount of time. The color of a star is an indicator of the star's surface temperature. In 1913, Henry Norris Russell, an American astronomer from Princeton University, created a graph of stars' spectral types to their luminosities[1]. Spectral types of stars are a way to classify the color of stars.

Spectral classification is the categorization of stars based on their properties. Annie J. Cannon categorized stars based on temperature. Spectral type is categorized into letters, OBAFGKM (hottest to coolest). Stars are also classified by their luminosities. Roman numerals denote luminosity classes. Class I stars are supergiants; class II stars are extreme giants; class III stars are giants; class IV stars are sub-giants; class V stars are dwarfs; class VI stars are sub-dwarfs; and class VII stars are white dwarfs[2].

The H-R diagram needs two variables of temperature and luminosity. Astronomers measure luminosity using apparent magnitude, which is the brightness of a star observed from Earth because the star of a certain brightness looks different from different distances. Even if two stars have the same luminosity, the closer star has a higher apparent magnitude.

To find the temperature of a star, astronomers look into the color of stars. A star's color is the difference between magnitudes when seen through different filters. Filters only allow specific wavelengths to be seen. Many H-R diagrams use B-V when the magnitude from the yellow filter is subtracted from the magnitude from the blue filter.

An H-R diagram plots the luminosity of stars on the y-axis. The brighter stars are further from the x-axis and the dimmer stars are closer to the x-axis. However, if the magnitude is set as the y-axis, brighter stars will be closer to the x-axis because brighter stars have lower magnitudes. The H-R diagram plots temperature or color on the x-axis. Usually, hotter stars are plotted near the y-axis, and cooler stars are plotted further away. As temperature decreases, B-V values increase.

As seen in Figure 1, stars on the H-R diagram can be classified into four groups. The first group is the line of points across the center in an inversely proportional direction. This group is called the "main sequence," accounting for 90

The stars above and slightly to the right of the main sequence, there are two groups: giants and supergiant stars. Supergiants are above the giants as they are brighter and emit more light. These stars are older stars that ran out of hydrogen, so they use heavier elements as fuel. These stars have low surface temperatures, but high luminosities. Due to the Stefan-Boltzmann law, they have large radii. Giant stars have a radius of 10 to 100 solar radii and are usually 10 to 1000 times more luminous than the Sun. Supergiants' radii are 30 to 500 solar radii. They have short lifespans due to their mass of 10 to 70 solar masses. Giants and supergiants account for most of the bright stars on the H-R

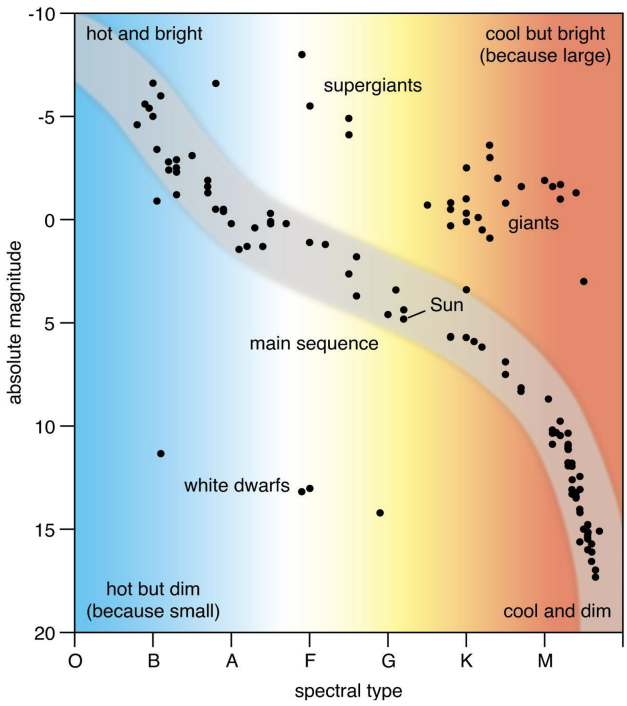

Fig. 1 This H-R diagram shows the different groups of stars within the H-R diagram[3].

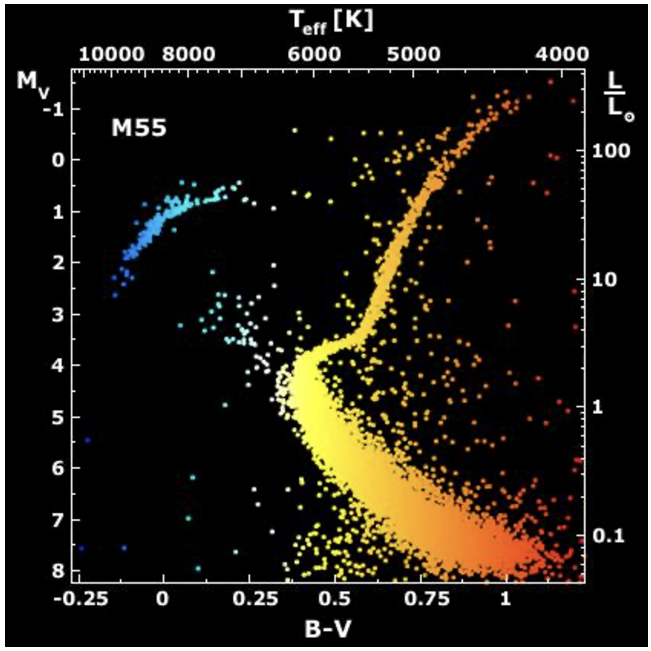

Fig. 2 This is the H-R diagram for globular star cluster M55[4].

diagram.

The stars below and slightly left of the main sequence belong to white dwarfs. These stars are giant stars that collapsed because they burned all their fuel. The light from these stars are remains of energy from the collapse. These stars are very hot but have low luminosity as they are small. White dwarfs have a similar mass to the Sun, but their volume is similar to the Earth. White dwarfs only account for 6% of all stars in the solar neighborhood, so they are less frequent on H-R diagrams.

The H-R diagram shows many things. It shows how the luminosity of a star is proportional to the mass of the star. It also shows the relationship between the color and temperature of stars. The reddish the stars are, the cooler they are. However, the bluer they are, the hotter they are. The H-R diagram shows the life cycle of a star. A star spends most of its life in the dense main sequence stage. As it runs out of hydrogen for fuel, it becomes a giant star for most of its life. Eventually, towards the end of its life, the giant star will explode into a supernova or become a white dwarf.

H-R diagrams drawn for different galaxy parts have different groups of stars. For example, the globular cluster H-R diagram differs starkly from stars around our galaxy as seen in Figure 2. Globular clusters are stars bound by gravity that are smaller than galaxies. In the H-R diagram for globular clusters, clusters show no stars in type O, B, or A of the main sequence. The lower right side of the main sequence is very dense. Also, there are a lot of stars in the giant regions.

Astronomers use the H-R diagram to measure a star cluster's distance from Earth. Astronomers could approximate how far the star cluster was by comparing the apparent magnitudes and absolute magnitudes with the distances of certain stars. This method is called "main sequence fitting" because the diagram was shifted up and down to fit the line with the main sequence on the HR diagram as seen in Figure 3.

Astronomers continue to study and create H-R diagrams to predict and anticipate more accurately about stars further into space. Using data from newer probes and satellites, astronomers can predict properties of stars that are far beyond our galaxy. Understanding more stars allows astronomers to understand more about the creation of stars and galaxies, ultimately the universe.

Theory of Beehive Cluster

The Beehive Cluster is intriguing because it has a lot of bright stars densely centralized, as seen in Figure 4, due to mass segregation. This phenomenon occurs in gravitationally bound systems, where big bright stars move towards the center. It is an open cluster that is only 577 light years away from Earth, making it one of the closest open clusters to Earth. The cluster has an apparent magnitude of 3.7 and is visible by the naked eye under good conditions[7]. Because the Beehive Cluster is so bright, it has been known to mankind since ancient times. In

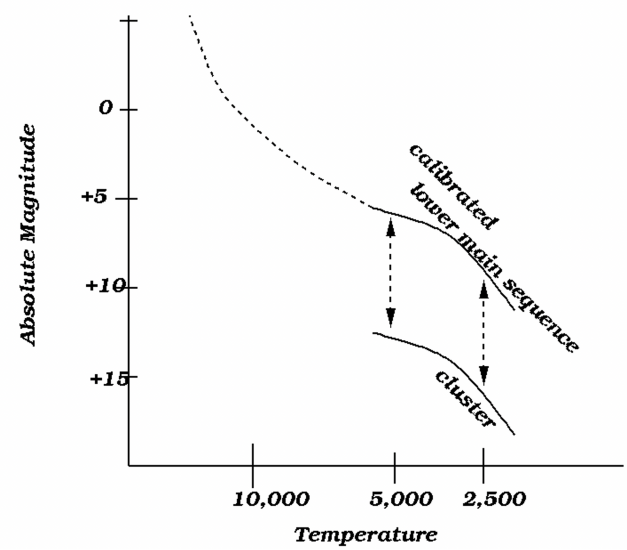

Fig. 3 This is a graph where the main sequence calibrated is plotted next to the hypothetical main cluster[5].

Fig. 4 Photo of the Beehive Cluster (M44)[6]

2012, scientists found 2 planets orbiting two stars in the cluster. These two planets and stars are similar to Jupiter and the Sun[8]. Furthermore, it is part of the constellation Cancer, which can be seen most clearly from February to May. Galileo Galilei studied this cluster and was able to find 40 stars. After finding its position in space, Charles Messier added it to his Messier catalog. In 1894, Wilhelm Schur drew a map of the cluster[9]. So far, there have been five giant stars and eleven white dwarfs identified in the cluster[10].

Sources of Data

All the data used for this study was obtained from the Gaia database. The Gaia database was queried using SQL and obtained 801 stars that were within the circle with a radius of 47.5 arc minutes[11] around an approximate center of the Beehive cluster (130.09, 19.67), which was found by using Sloan Digital Sky Survey's navigation tool. The following data has been extracted.

Excel was used to handle calculations on the average, maximum, minimum, range, median, and standard deviation of the data from Table 1. The calculated values are shown in Table 2.

Results

H-R Diagram of M44

The magnitudes of the mean magnitudes of the stars in the integrated RP, BP, and G bands from the extracted data are apparent magnitudes, and brightness if measured from the Earth. To create an H-R diagram, absolute magnitudes, and brightness if measured from the standard distance of 10 parsecs, are needed. Using absolute magnitude is important because it allows the luminosity of stars to be compared with one another while disregarding their distance from the Earth. Using absolute magnitude, the H-R diagram can represent an intrinsic luminosity for the spectral type of stars.

To find the star's absolute magnitude, the star's distance must be calculated first. When p is the arcseconds of the parallax value, the distance formula is d=1/p. When p is the milliarcseconds (mas) of the parallax value, the formula is converted to d=1000/p.

While Gaia provides highly accurate parallax measurements, these measurements are susceptible to various sources of error, including systematic effects, instrumental limitations, and astrometric model uncertainties. Systematic errors can arise from calibration issues or unresolved binary stars, and instrumental factors such as detector noise and optical distortions can also affect the precision of the parallax data. Additionally, the astrometric model used to derive parallaxes involves simplifications that may not hold true for all stars. These errors can impact the accuracy of our distance estimates and, consequently, the derived absolute magnitudes and the H-R diagram.

After calculating the distance, the absolute magnitudes can be calculated. The formula for absolute magnitude is M=m-5log(d)+5. M denotes the absolute magnitude and m denotes the apparent magnitude. The H-R diagram can be made now that the absolute magnitude has been calculated. Figure 5 shows the H-R diagram that has been created using the absolute magnitude through the G band.

Data	Definition and Explanation
Right Ascension	Barycentric right ascension α of the source in ICRS at the reference epoch
Declination	Barycentric declination δ of the source in ICRS at the reference epoch
BP - RP color	Magnitude of BP subtracted by magnitude of RP.
Integrated RP mean magnitude	Mean magnitude in the integrated RP band. This is computed from the RP-band mean flux applying the magnitude zero-point in the Vega scale.
Integrated BP mean magnitude	Mean magnitude in the integrated BP band. This is computed from the BP-band mean flux applying the magnitude zero-point in the Vega scale.
Integrated G mean magnitude	Mean magnitude in the integrated G band. This is computed from the G-band mean flux applying the magnitude zero-point in the Vega scale.
Proper motion in right ascension	Proper motion in right ascension $\mu_\alpha^* \equiv \mu_\alpha \cos\delta$ of the source in ICRS at the reference epoch. This is the local tangent plane projection of the proper motion vector in the direction of increasing right ascension.
Proper motion in declination	Proper motion in declination μ_δ of the source at the reference epoch. This is the projection of the proper motion vector in the direction of increasing declination.
Parallax	Absolute stellar parallax ϖ of the source at the reference epoch
Radial Velocity	Spectroscopic radial velocity in the Solar system barycentric reference frame.

Table 1 Definition and Explanation of Data Collected[12]

	Average	Maximum	Minimum	Range	Median	Standard Deviation
Right Ascension (in degrees)	130.0339	130.9124	129.2534	1.6589	130.0260	0.4040
Declination (in degrees)	19.6594	20.4334	18.8848	1.5486	19.6566	0.3902
BP - RP color	1.0415	2.7809	0.0206	2.7603	0.8981	0.4691
Integrated RP mean magnitude	12.4283	14.5335	5.5203	9.0132	12.8939	1.6554
Integrated BP mean magnitude	13.4699	17.2667	6.5928	10.6738	13.9139	1.8859
Integrated G mean magnitude	13.0235	15.9900	6.1524	9.8374	13.5088	1.7500
Proper motion in right ascension (in mas/yr)	-12.5103	48.9265	-107.2468	156.1733	-6.7870	18.0694
Proper motion in declination (in mas/yr)	-10.0913	39.5366	-179.5104	219.0471	-9.3197	16.2690
Parallax (in mas)	2.8465	14.3834	-1.4395	15.8230	2.0420	2.1968
Radial Velocity (in km/s)	22.7470	137.8984	-122.1055	260.0039	31.2416	32.1480

Table 2 Statistics on Data Collected

The H-R diagram of M44 shows the different types of stars in the cluster. The diagram has a main sequence from the top left to the bottom right. The group of 5 stars, 4 stars below the main sequence between 0.7 to 1.1 in BP-RP color, and the star near the 1.5 BP-RP color below the main sequence, are all most likely white dwarf stars. The group of four white dwarf stars are probably of different ages in stellar evolution compared to the one white dwarf star with lower brightness. The number of white dwarfs in M44 has been a point of contention. According to Casewell in "High-resolution optical spectroscopy of Praesepe white dwarfs", there could be anywhere from 5-11 white dwarfs in M44 that we can verify[13]. There are a lot of stars above the main sequence between 1 to 1.3 BP-RP color, which are most likely giants. This set of giants creates a trend line that is perpendicular to the main sequence. Within the area surrounded by the main sequence and the trend line of the giants, there are few stars, which can be determined to be supergiants. They have lower BP-RP color, but much higher brightness.

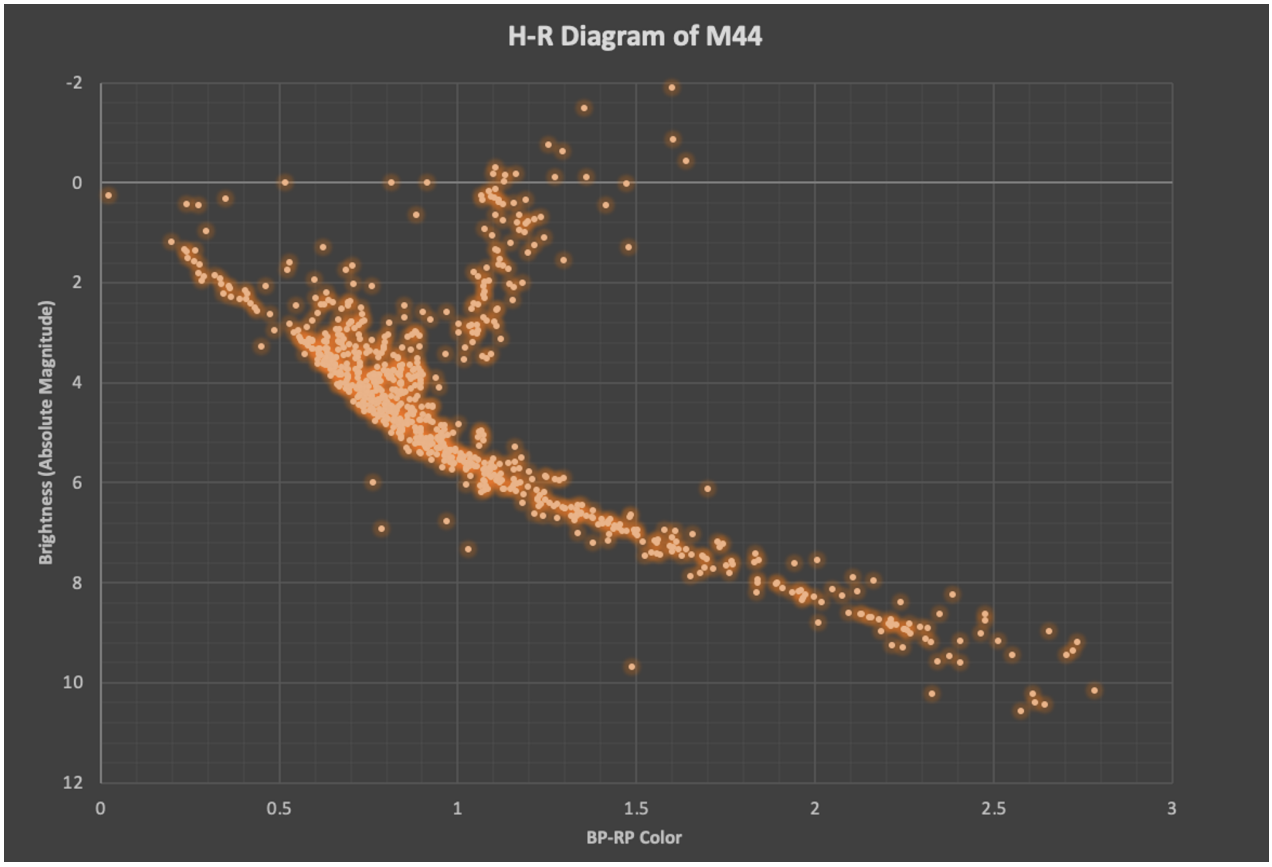

Fig. 5 H-R Diagram of M44

Isochrones

The Isochrone Generator[14] from the Dartmouth Stellar Evolution Database was used to find isochrones. For the abundance of iron against hydrogen, [Fe/H], the value of +0.12 ±0.04[15] was used based on Ann Merchant Boesgaard's paper on the chemical composition of M44. The abundance of iron against hydrogen is an indicator of metallicity, which affects the opacities in stellar interiors. This influences the luminosity and temperature of stars. Higher metallicity generally leads to higher opacities, resulting in cooler and more luminous stars. An incorrect assumption about metallicity could shift the isochrones, leading to inaccurate age estimations. Another important value is the helium mass fraction. The value of 0.245+1.5*Z was used for the helium mass fraction. This value influences stellar evolution timescales and eventually the position of stars on the H-R diagram. Higher helium fraction accelerates stellar evolution, leading to earlier phases of helium burning. Incorrect values about the helium content can lead to inaccurate fits of the isochrones to the observed data. For each isochrone, the isochrones were superimposed onto the H-R diagram to see how well they fit with the diagram.

To create each isochrone, ages must be chosen, so the ages of 0.0 and 5.0 Gyr were chosen. After seeing both 0.0 and 5.0 Gyr isochrones superimposed onto the H-R diagram, it was clear that the age was between them. Therefore, the next isochrone test was 3.0 Gyr. The isochrone for 3.0 Gyr looked quite similar to the 5.0 Gyr isochrone. Isochrones less than 3.0 Gyr, such as 1.0 Gyr were tested. There was much change compared to the 3.0 and 5.0 Gyr isochrones, so 0.5 Gyr isochrone was tested. After comparing the isochrone fits for 0.5 and 1.0 Gyr, it was clear that the best-fitting isochrone would have the age between those two ages, so ages from 0.5 to 1.0 Gyr in intervals of 0.1 Gyr were all tested.

After looking at isochrones of the age of 0.6, 0.7, 0.8, and 0.9 Gyr, it can be predicted that the best-fitting isochrone would be around the age of 0.7 Gyr, as shown in Figure 6. To make sure that 0.7 Gyr was the best-fitting isochrone, we used Python to compute the Root Mean Squared Error (RMSE)and Mean Absolute Error (MAE) values for each isochrone.

To write the code, the data was first prepared so that the observed data and the isochrone were formatted in pairs of BP-RP Color and Absolute Magnitude. Then, for each observed data point, the nearest isochrone point was found in terms of BP-

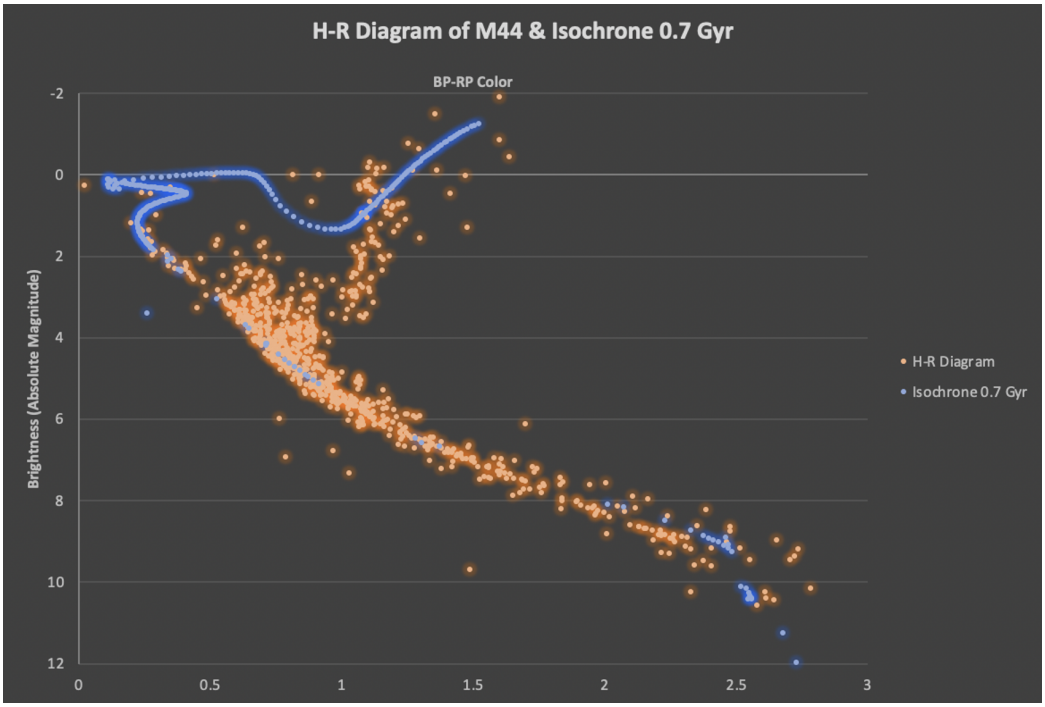

Fig. 6 H-R Diagram of M44 0.7 Gyr Isochrones superimposed

RP Color. Then, the difference in absolute magnitude between the observed data point and its nearest isochrone point was computed. After that, we proceeded with the RMSE and MAE value calculations.

The isochrone of 0.7 was indeed the best fit with an RMSE value of 0.24054768705802107 and an MAE value of 0.15738009607558145. Isochrone of 0.7 had significantly lower RMSE and MAE values than isochrone of 0.6 and isochrone of 0.7. As lower RMSE and MAE values indicate a better fit, 0.7 Gyr was determined to be the age of the cluster.

Distance Range Implementation

As seen in the isochrone graphs that have been superimposed onto the H-R diagram, there are a lot of stars above the main sequence between the BP-RP Color of 0.5 and 1. After manipulating some data types, it was found that parallax and distance determined those data points.

Creating a range of distance limits the stars from outside the cluster to being part of the study. As the distance is correlated with the parallax of the cluster, distance can also be limited by putting a range on the parallax. Stars may be in the same direction but at different distances away.

There are varying distances cited for the M44, most sources cite it between 125[16] and 187[17] parsecs. Using this range of distance, the recalculated average parallax would be 5.57 mas. This parallax value lies within the error range of the parallax calculations of 5.21 ± 0.79 done by George Gatewood and Joost Kiewiet de Jonge using the Allegheny Observatory at the University of Pittsburgh in 1993. Gatewood and de Jonge's calculations used trigonometric parallax measurements[18]. After implementing that range of distance, the following H-R diagram can be made.

Figure 7 only includes 172 stars. The main sequence is visible. There seems to be one white dwarf where the BP-RP color is 1.5 and the absolute magnitude of brightness is around 10. Three stars that seem to be giants are between the BP-RP color of 1 and 1.5 and have an absolute magnitude of brightness of around 0. There is also an additional star at around 0.5 BP-RP color above the main sequence that is a giant. This result lines up well with Kraus and Hillenbrand's estimation in "The Stellar Populations of Praesepe and Coma Berenices" that there are five giant stars, with four having spectral class K0 III and the fifth with G0 III[19]. Our H-R diagram finds three of the four giants in the K0 III spectral class and the singular giant in the G0 III spectral class.

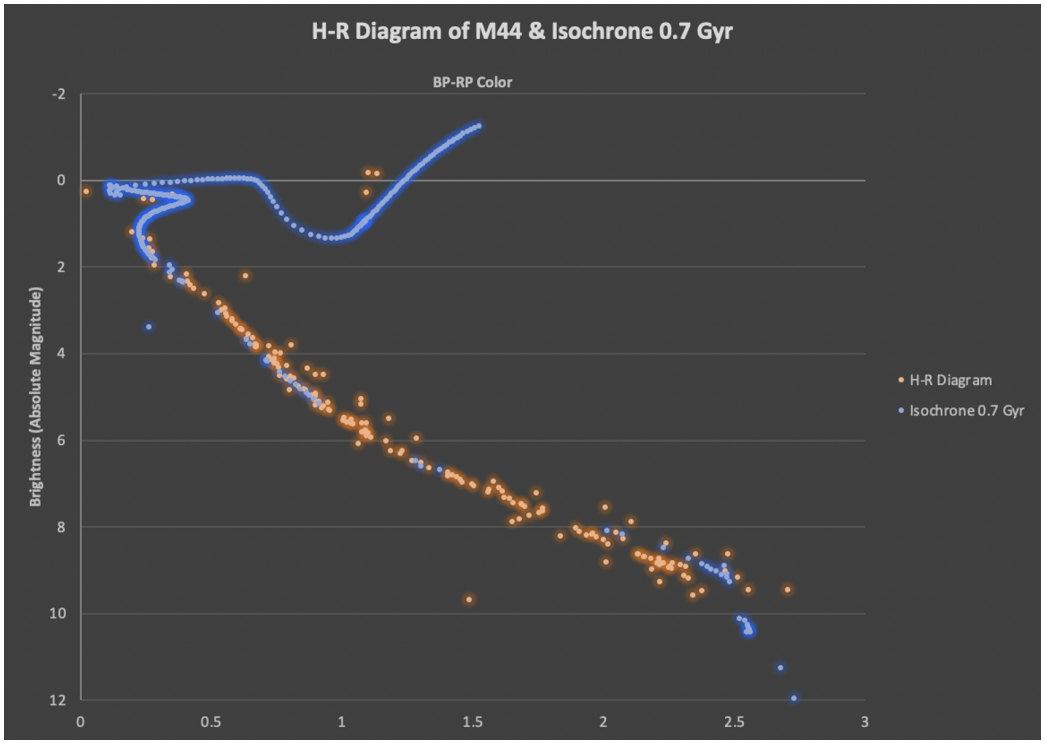

Fig. 7 Revised H-R Diagram of M44 with 0.7 Gyr Isochrones superimposed

Virial Theorem and Mass

The mass of the cluster can be found using the virial theorem. The following is the virial theorem:

$$\langle KE \rangle = -\frac{1}{2}\langle GPE \rangle \quad [20] \tag{1}$$

KE represents the kinetic energy and GPE represents gravitational potential energy.

The standard deviation of the radial velocity is velocity dispersion, which is denoted as σ. The average one-dimensional velocity is denoted as v_{1D}. The relationship between those two variables is the following:

$$v_{1D}^2 = \sigma_r^2 \tag{2}$$

The average three-dimensional velocity is denoted as v_{3D}, leading to the following relationship:

$$v_{3D}^2 = 3v_{1D}^2 = 3\sigma_r^2 \tag{3}$$

Kinetic energy can be estimated with the following equation:

$$\langle KE \rangle = \frac{1}{2}mv^2 = \frac{1}{2}m(3\sigma_r^2) \tag{4}$$

Gravitational potential energy can also be estimated to be:

$$GPE = -\frac{GMm}{r} \tag{5}$$

By assuming the distance between the center of mass and an average star to be half the radius of the cluster, the following equation can be made:

$$\langle GPE \rangle \approx -\frac{GMm}{\frac{1}{2}R} \tag{6}$$

where R is the radius of the cluster and G is the gravitational constant.

When combined, the following equation can be formed:

$$\frac{1}{2}m(3\sigma_r^2) \approx \frac{1}{2}\frac{GMm}{\frac{1}{2}R} \tag{7}$$

When solved for M, the following equation is obtained:

$$M = \frac{3\sigma_r^2 R}{2G} \tag{8}$$

Using the Gaia data with the distance range implemented, the velocity dispersion (σ_r) was calculated by finding the standard deviation of radial velocity, which was 18.115907 km/s.For this calculation, the radius of 5 parsecs was used as it was converted from the 47.5 arcmins that was used at the beginning of the data collection phase through SQL in the Gaia database. When all the constants and variables were substituted, the final mass of 572.417593 $M\odot$ was obtained.

These constants play a significant role in the mass calculation as the mass is directly proportional to the radius and proportional to the square of the velocity dispersion. To assess the sensitivity of the mass estimate to variations in cluster radius and velocity dispersion, we conducted a sensitivity analysis. A 10% increase in radius from 5 parsecs to 5.5 parsecs results in a mass estimate of approximately 629.66 $M\odot$, while a 10% decrease to 4.5 parsecs results in a mass estimate of approximately 515.17 $M\odot$. Similarly, a 10% increase in velocity dispersion to approximately 19.927 km/s results in a mass estimate of approximately 692.63 $M\odot$, whereas a 10% decrease to approximately 16.305 km/s results in a mass estimate of approximately 460.90 $M\odot$.

Discussion

Robert J. Vanderbei, an American professor at Princeton University, created an H-R diagram of the M44 cluster as seen in Figure 8.

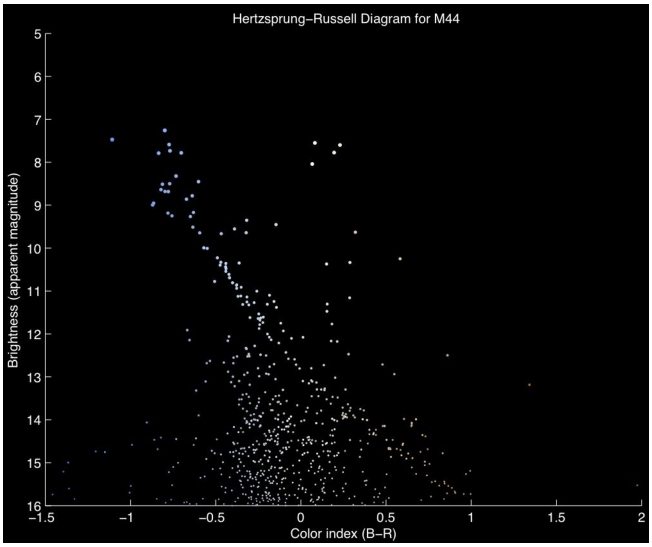

Fig. 8 Vanderbei's H-R Diagram for M44 [21]

The biggest difference between the H-R diagram Dr. Vanderbei created and this study's diagram is the y-axis. Vanderbei used apparent magnitude while this study used an absolute magnitude. In the context of the H-R diagram, using absolute magnitude categorizes and compares stars based on their true properties. If apparent magnitude is used, the distances of the stars would skew the results. A very bright star far away might have the same apparent magnitude as a dimmer star closer to us. Using absolute magnitude, stars can be accurately plotted based on their inherent brightness and temperature, which can help better understand their life cycles and the relationship between different types of stars. The data used in this study, the result is quite different, as seen in Figure 9.

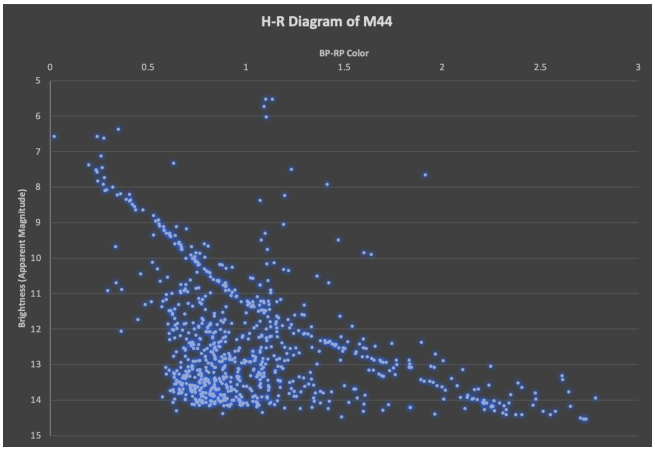

Fig. 9 H-R Diagram for M44 using Apparent Magnitude for Brightness

First, in the graph directly above, all data points are on the positive side of the x-axis. However, for Vanderbei's graph, many are also on the negative side. The graph above seems to be translated by 1 to the right from Vanderbei's graph. For the y-axis, Vanderbei's graph is slightly below the graph above, meaning the graph above looks translated by 2 upwards from Vanderbei's graph.

This study used an absolute magnitude because of the excessive data points. The group of stars below the main sequence may be present due to the lack of refining of the parallax/distance values. However, on the absolute magnitude diagram, those points represent the various stars of M44 better.

We can also compare our further calculations with previous studies. According to "Age Determinations of the Hyades, Praesepe, and Pleiades via MESA Models with Rotation" in The Astrophysical Journal, researchers estimate the age of Praesepe as 680 Myr, which is 0.68 Gyrs [22]. This is very close to the estimate of 0.7 Gyrs we obtained using the isochrone fitting technique. Also, Kraus and Hillenbrand calculate in "The Stellar Populations of Praesepe and Coma Berenices" that they estimated the mass of Praesepe to be 550 ± 40 $M\odot$ [23]. They used a method that found 1010 candidate members of the cluster and analyzed the role of mass segregation and tidal stripping to calculate the mass. They used data from the Two Micron All Sky Survey (2MASS) and the Sloan Digital Sky Survey (SDSS). The value we obtained, using the virial theorem, was 572.417593 $M\odot$, which is within their range of mass for the Praesepe. Before applying the distance range, the average distance was 786.0481 ps; however, after the distance range was applied, the average distance was 180.2552. Loktin and Matkin estimate Praesepe to be 175 ± 47 pc away [24].

Conclusion and Future Perspective

This research on the Praesepe star cluster (Beehive Cluster, M44) using the H-R diagram has provided valuable insights into the cluster's properties. Our analysis determined the final mass of the cluster to be approximately 572.4 $M\odot$, with an estimated age of 0.7 Gyr. The average distance was estimated to be 180.2552 parsecs with around five white dwarfs and four giants. These findings contribute to a deeper understanding of M44's structure and stellar dynamics.

Although there were not many H R diagrams of the M44 made in the past, the diagram was quite successful when evaluated with Vanderbei's diagram. Using absolute magnitude made it easier to compare with H-R diagrams of other clusters to find what type of stars were in the cluster and how old they were. The absolute magnitude H-R diagram helped to classify the stars based on their true properties, which allowed for accurate analysis of their luminosity and temperature.

We compared the results with previous studies to validate the findings and identify any discrepancies. For example, our estimated age of the Praesepe was 0.7 Gyr, closely aligning with the 0.68 Gyr reported by Gossage et al. (2018). Similarly, our mass estimate of 572.417593 $M\odot$ falls within the range of 550 ± 40 $M\odot$ estimated by Kraus and Hillenbrand (2007). These consistencies reinforce the reliability of our methods.

However, some discrepancies were noted. For example, the number of identified white dwarfs varied across studies, with our identification of five white dwarfs aligning with the lower end of the range suggested by Casewell et al. (2009), who reported between 5 and 11 white dwarfs. Such discrepancies could be due to differences in data quality, selection criteria, or observational techniques. These inconsistencies highlight the need for further investigation and methodological refinement.

Our plans for further research include extending the study to include more clusters, providing a broader perspective. By comparing these clusters, we can investigate the influence of different environments on stellar evolution and determine whether similar patterns emerge across diverse clusters. Additionally, improving the accuracy of distance measurements is crucial. We plan to use methods such as spectroscopic distance indicators, which can offer more precise distance estimations, leading to improved cluster mass and age estimations.

Moreover, it is important to explore other models that take into account other factors that influence stellar properties, such as stellar rotation and magnetic activity. They can provide a more nuanced understanding of our calculations. Also, investigating the chemical composition of stars can reveal new insights into the star formation process and the interplay between a star's initial composition and its eventual fate.

Through this extended study, we hope to deepen our understanding of star clusters and stellar evolution. This can contribute significantly to the broader field of astronomy, enhancing our knowledge of the universe's structure and the processes that shape it.

Acknowledgments

I would like to thank Dr. Shyamal Mitra for his guidance and inspiration throughout this paper.

References

1 *The Hertzsprung-Russell Diagram*, http://skyserver.sdss.org/dr7/en/proj/advanced/hr/, Accessed: 2023-05-21.

2 *Pulsating Variable Stars and the Hertzsprung-Russell (H-R) Diagram*, http://chandra.harvard.edu/edu/formal/variable_stars/bg_info.html, Accessed: 2023-05-21.

3 *Hertzsprung-Russell Diagram: Cosmos*, http://astronomy.swin.edu.au/cosmos/h/hertzsprung-russell+diagram, Accessed: 2023-05-21.

4 B. J. Mochejska and J. Kaluzny, *APOD: - M55 Color Magnitude Diagram*, http://apod.nasa.gov/apod/ap010223.html, 2001.

5 G. Bothun, *2.3.2. The Second Rung: Distances to Stellar Clusters*, http://ned.ipac.caltech.edu/level5/Bothun2/Bothun2_3_2.html, Accessed: 2023-05-21.

6 *Bees in the Beehive*, http://www.jpl.nasa.gov/images/pia15801-bees-in-the-beehive, 2012.

7 Admin, *Messier 44: Beehive Cluster*, http://www.messier-objects.com/messier-44-beehive-cluster/, 2022.

8 B. McClure and D. Byrd, *The Beehive Cluster: A Swarm of 1,000 Stars*, http://earthsky.org/clusters-nebulae-galaxies/praesepe-beehive-cluster/, 2023.

9 H. Frommert, *Messier Questions & Answers*, http://www.messier.seds.org/m/m042.html, Accessed: 2023-05-21.

10 P. D. Dobbie, R. Napiwotzki, M. R. Burleigh and et al., *Monthly Notices of the Royal Astronomical Society*, 2006, **369**, 383–389.

11 britastro.org, *Close Approach of the Moon and M44*, http://britastro.org/event/close-approach-of-the-moon-and-m44-4, 2019.

12 Gaia_source, *Gaia_source*, http://gea.esac.esa.int/archive/documentation/GEDR3/Gaia_archive/chap_datamodel/sec_dm_main_tables/ssec_dm_gaia_source.html, Accessed: 2023-05-21.

13 S. L. Casewell and et al., *Monthly Notices of the Royal Astronomical Society*, 2009, **395**, 1795–1804.

14 *Isochrone and LF Generator*, http://stellar.dartmouth.edu/models/isolf_new.html, Accessed: 2023-05-21.

15 A. Boesgaard, B. Roper and M. Lum, *The Astrophysical Journal*, 2013, **775**, year.

16 D. J. Pinfield and et al., *Monthly Notices of the Royal Astronomical Society*, 2003, **342**, 1241–1259.

17 *What's up: How to Star Hop*, http://cosmoquest.org/x/2022/02/whats-up-how-to-star-hop/, 2022.

18 G. Gatewood and J. Kiewiet De Jonge, *Astrophysical Journal, Part 1*, 1994, **428**, 166–169.

19 A. L. Kraus and L. A. Hillenbrand, *The Astronomical Journal*, 2007, **134**, 2340.

20 M. Richmond, *Using the Virial Theorem: Mass of a Globular Cluster*, http://spiff.rit.edu/classes/phys440/lectures/glob_clus/glob_clus.html, Accessed: 2023-05-21.

21 R. J. Vanderbei, *M44 — the Beehive Cluster*, http://vanderbei.princeton.edu/images/NJP/m44.html, Accessed: 2023-05-21.

22 S. Gossage and et al., *The Astrophysical Journal*, 2018, **863**, 67.

23 A. L. Kraus and L. A. Hillenbrand, *The Astronomical Journal*, 2007, **134**, 2340.

24 A. V. Loktin and N. V. Matkin, *Astronomische Nachrichten*, 1989, **310**, 231.